A Study on the Coexistence of Fixed Satellite Service and Cellular Networks in a mmWave Scenario

Francesco Guidolin[†*]   Maziar Nekovee[*]   Leonardo Badia[†]   Michele Zorzi [†]

† Dept. of Information Engineering, University of Padova, via Gradenigo 6/B, 35131 Padova, Italy

* Samsung R&D Institute UK, Communications House, South Street, Staines-upon-Thames.Surrey TW18 4QE, UK

Abstract—The use of a larger bandwith in the millimeter wave (mmWave) spectrum is one of the key components of next generation cellular networks. Currently, part of this band is allocated on a co-primary basis to a number of other applications, such as the fixed satellite services (FSSs). In this paper, we investigate the coexistence between a cellular network and FSSs in a mmWave scenario. In light of the parameters recommended by the standard and the recent results presented in the literature on the mmWave channel model, we analyze different BSs deployments and different antenna configurations at the transmitters. Finally, we show how, exploiting the features of a mmWave scenario, the coexistence between cellular and satellite services is feasible and the interference at the FSS antenna can be kept below recommended levels.

Index Terms—*Millimeter wave communication; cellular networks; radio spectrum management; satellite communication; beamforming.*

I. INTRODUCTION

One of the primary contributors to global mobile traffic growth is the increasing number of wireless devices that are accessing mobile networks. Each year, several million new devices with different form factors and increased capabilities are being introduced. Over half a billion (526 million) mobile devices and connections were added in 2013 and the overall mobile data traffic is expected to grow to 15.9 exabytes per month by 2018, nearly an 11-fold increase over 2013 [1]. One of the most promising technologies to support the fast growing demand of high rate connectivity in next generation mobile cellular networks is the use of wide bands in millimeter wave (mmWave) frequency ranges. In particular, cellular allocations today are largely constrained under 6 GHz but it will be possible to obtain a spectrum 200 times greater by exploiting the frequencies between 20 and 300 GHz.

Recent studies demonstrate the feasibility of mmWave mobile communications using multiple antenna arrays in conjunction with adaptive beamforming in order to compensate far propagation losses at high frequencies [2]. Some experimental results obtained using a prototype developed by Samsung are reported in [3]. The small wavelengths of these frequencies (in fact, of the order of 10^{-3} m) allow to use large arrays of antennas to support directional beams to the users. A hybrid analog-digital beamforming scheme that exploits the mmWave channel and an antenna array with a low implementation complexity is presented in [4], and several measurements and

capacity studies recently performed in New York City at 28 and 73 GHz are presented in [5]. These studies are used in [6][7] to develop statistical channel models including pathloss, number of spatial clusters, angular dispersion and outage probability. In general, even in non-line-of-sight scenarios, strong signals can be detected 100 to 200 m from the base station (BS) and spatial multiplexing can be supported. Similar channel models based on indoor and outdoor measurements are presented in [8].

One of the candidate bands for the deployment of mmWave cellular mobile networks is the portion of spectrum between 17 and 30 GHz. Currently, part of this band is allocated on a co-primary basis to fixed services (FSs), cellular network backhaul, and fixed satellite services (FSSs) [9]. FSS is the official classification for geostationary communications satellites that provide, for instance, broadcast feeds to television stations, radio stations and broadcast networks. The FSS uplink (from FSS to satellite) is allocated in the band from 27.5 to 30 GHz and the downlink (from satellite to FSS) is allocated from 17.3 to 21 GHz [10]. Fig. 1 shows the spectrum allocations of the FSSs and high density FSSs (HDFSS) designated by the International Telecommunication Union (ITU) [10]. Therefore, it is important to study the possible coexistence between FSSs and mmWave cellular base stations (BSs) in order to preserve the functionalities of the satellite services.
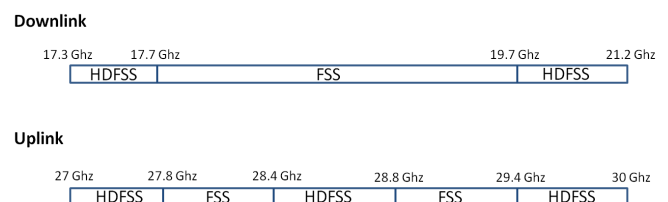

Fig. 1. FSSs and HDFSSs spectrum allocation

ITU investigated the spectrum sharing between FSSs and IMT-advanced systems in the frequency band from 3.4 to 6.4 GHz considering the devices as primary and secondary users respectively [11][12]. The aim of these works is to evaluate the interference at the FSS and to design possible interference mitigation techniques able to guarantee a minimum signal to interference ratio (SIR) at the primary user. Several techniques can be applied to mitigate the interference towards the FSS and improve the BS-FSS coexistence. Some cognitive Sat-

Coms underlay, interweave and database related techniques to manage the BS-FSS interference are presented in [13]. An interference mitigation technique based on a nullsteering multi-user multiple-input-multiple-output (MU-MIMO) spatial division access scheme for frequency sharing between an IMT-advanced system and FSSs is proposed in [14]. A study on the separation distance between geostationary satellite communications (GSO) and terrestrial network in Ka band that guarantees a fixed interference to noise level (I/N) at the primary receiver is presented in [15]. A transmit beamforming technique at the BS to maximize the signal to interference plus noise ratio (SINR) towards the desired secondary user and to mitigate the interference towards the primary satellite terminals is proposed in [16].

Differently from this literature, in our work we study the coexistence between FSSs and mobile cellular BSs in the mmWave bands. In particular, we consider the parameters and the FSSs radiation pattern provided by the ITU and the channel models provided by the literature in these frequency bands. We analyze the level of I/N at the FSS considering various multiple antenna configurations at the BS and different deployments of the mobile transmitters when no cooperation is allowed between the BSs. In particular, starting from the lower bound, represented by an omnidirectional configuration of the transmitters, we extend our work to the analysis of large antenna arrays that will be used in the new generation of mobile cellular systems. Finally, we show that exploiting a large number of antennas at the BSs and properly setting the protection distance between FSS and mobile BS, coexistence between the two systems is feasible.

The paper is organized as follows. Section II describes the model considered, focusing on the standard system parameters used in the analysis and Section III gives the performance evaluation for the different scenarios considered. Finally, conclusions and future works are drawn in Section IV.

Remark: Throughout the paper, we use boldface letters for vectors and matrices, and we denote with $(\cdot)^T$ the conjugate transpose.

II. SYSTEM MODEL

In this paper we consider the frequency allocation at 18 GHz that corresponds to the downlink band of the FSS system. The scenario is depicted in Fig. 2. We define as *primary link* the transmission from the satellite to the FSS while as *secondary link* the connection from a cellular BS to a mobile user equipment (UE) is considered. An additional *interfering link* is present from the BS to the FSS. A scheduling algorithm for this scenario has been proposed and studied in [17].

We can compute the interference (on a log scale) generated on such a link by BS n to the FSS as

$$I_n = P_{BS} + G_{FSS}(\phi) + G_{BS} - L(d) \tag{1}$$

where P_{BS} is the BS transmission power, $G_{FSS}(\phi)$ is the FSS antenna gain in the direction ϕ, G_{BS} is the BS antenna gain, ϕ is the angle between the main FSS antenna lobe and BS n, and $L(d)$ is the pathloss component at distance d, which in turn is the FSS-BS distance.
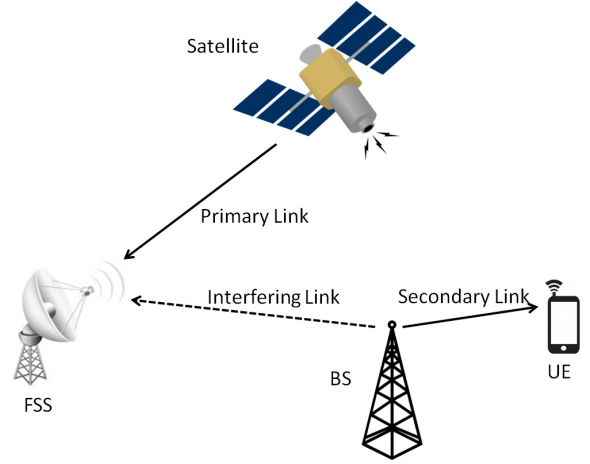

Fig. 2. FSS-BS coexistence scenario

The FSS antenna gain is computed as a function of the off-boresight angles, which can be calculated using the model in [18]. Considering ϑ as the azimuth of the BS w.r.t. the FSS Rx main lobe, the off-boresight angle ϕ of the BS towards the FSS can be calculated as

$$\phi = \arccos(\cos(\alpha)\cos(\epsilon)\cos(\vartheta) + \sin(\alpha)\sin(\epsilon)) \tag{2}$$

where α is the FSS elevation angle and ϵ is computed as:

$$\epsilon = \frac{h_t - h_s}{d} - \frac{d}{2r} \tag{3}$$

where h_s and h_t are the heights of the BS and the FSS in meters, respectively, while r is the effective Earth radius ($\approx 8.5 \cdot 10^6$ m). The FSS off-boresight antenna gain pattern in dB can be computed as [19]:

$$G_{FSS}(\phi) = \begin{cases} G_{max} & if\ 0° < \phi < 1° \\ 32 - 25\log\phi & if\ 1° \leq \phi < 48° \\ -10 & if\ 48° \leq \phi \leq 180° \end{cases}$$

where G_{max} is the main beam axis FSS antenna gain.

Since mmWave channels are expected to have limited scattering, we adopt a double-directional geometry based stochastic model with L scatterers [20]. Assuming N_{UE} antennas at the UE and N_{BS} antennas at the BS the $N_{UE} \times N_{BS}$ channel matrix $\mathbf{H}$ can be computed as

$$\mathbf{H} = \sqrt{\frac{N_{BS}N_{UE}}{L}} \sum_{\ell=1}^{L} \alpha_\ell \mathbf{a}_{UE}(\gamma_\ell^{UE})\mathbf{a}_{BS}^*(\gamma_\ell^{BS}) \tag{4}$$

where α_ℓ is the complex gain of the ℓth path and $\gamma_\ell^{UE}, \gamma_\ell^{BS} \in [0, 2\pi]$ are uniformly distributed random variables that represent the angles of arrival and departure, respectively. Finally, $\mathbf{a}_{UE}$ and $\mathbf{a}_{BS}$ are the antenna array responses at the UEs and BSs respectively. Assuming uniform linear arrays, $\mathbf{a}_{BS}$ can be written as

$$\mathbf{a}_{BS} = \frac{1}{\sqrt{N_{BS}}} \left[1, e^{j\frac{2\pi}{\lambda}D\sin(\gamma_l^{BS})}, ..., e^{j(N_{BS}-1)\frac{2\pi}{\lambda}D\sin(\gamma_l^{BS})} \right] \tag{5}$$

where D is the distance between antennas. Similarly, $\mathbf{a}_{UE}$ can be computed by substituting N_{BS} and γ_ℓ^{BS} in (5) with N_{UE} and γ_ℓ^{UE}, respectively.

We assume that the BS antenna gain in dB is

$$G_{BS} = G_{omni} + G_{BF} \tag{6}$$

where G_{omni} is the conventional antenna gain when no beamforming techniques are applied and G_{BF} is the beamforming gain. In this work, we adopt an RF beamforming where the gain is obtained by controlling phase and magnitude of the input signal to each antenna to form a directional beam in a particular direction. In order to reduce the system complexity, we assume that the BS can select the beam configuration within a predefined beam codebook with cardinality N_t that uniformly covers the azimuth directions around the BS. In particular, the codebooks at the transmitter and the receiver are formed by N_t and N_r weight vectors $\{\mathbf{v}_1, ..., \mathbf{v}_{N_t}\}$ $\{\mathbf{w}_1, ..., \mathbf{w}_{N_r}\}$ of sizes N_{BS} and N_{UE}, respectively. Each vector is computed as $\mathbf{v}_i = \mathbf{a}(\rho_i)$ and $\mathbf{w}_k = \mathbf{a}(\theta_k)$ where ρ_i and θ_k are the azimuth angles for the i-th transmit RF beam and k-th receive RF beam. We assume a multiple-input-single-output (MISO) scenario, in which the beamforming gain in the direction of the FSS antenna is:

$$G_{BF} = 10 \log(|\mathbf{v}_i^T \mathbf{h}_{FSS}|^2) \tag{7}$$

where $\mathbf{v}_i$ is the beamforming precoding vector selected by the BS and $\mathbf{h}_{FSS}$ is the channel matrix between the BS and the FSS.

Recommendation [21] indicates that interference from fixed service systems should not cause the BER to exceed 10^{-4} for more than 0.03% of any month nor cause the BER to exceed 10^{-3} for 0.005% of any month. These interference allowances, in terms of percentage of system noise, can be converted into corresponding values of I/N. For this percentage of time, referred in the literature as "short term" interference, the corresponding I/N values are equal to -2.4 and 0 dB, respectively. To evaluate the level of interference at the FSS we consider a "long term" interference criterion that refers to a percentage of time greater than 20%. In this case, recommendation [21] allows an interference level equivalent to 10% of the clear-sky satellite system noise that would give rise to a BER of 10^{-6}. The recommended I/N value is computed in [22] and is equal to -10 dB.

A. Scenarios Considered

We evaluate the interference at the FSS using three different scenarios.

In the first scenario we consider a **single BS** equipped with one omnidirectional antenna to evaluate the impact of the BS position and the elevation angle on the interference at the FSS. In this case, the BS antenna gain is given only by the omnidirectional component.

In the second scenario, we evaluate the aggregate interference from **multiple omnidirectional BSs** deployed in circular tiers around the FSS with fixed inter-site distance. The interference at the FSS is given by the sum of all the BS contributions that depend on the transmitter positions and on

the FSS elevation angle. We define as protection distance d_p the distance from the FSS and the first tier of BSs. The scenario is depicted in Fig. 3.
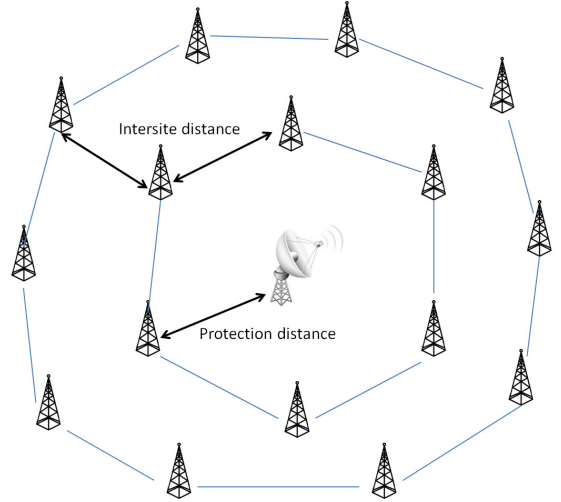

Fig. 3. Multiple BSs scenario

In the third scenario, we consider **multiple directional BSs**. In this case, the BSs, deployed as in the previous scenario, are equipped with multiple antennas and an RF beamforming scheme is adopted to serve the single antenna UEs. The users are randomly distributed within the BS coverage area and each BS selects one user at a time. The precoding beam vector is selected by each BS within the predefined beam codebook to maximize the SNR at the UE selected. We assume that the user scheduling and the beamforming selection are performed in a distributed manner among the BSs without any cooperation or signalling for interference coordination.

III. PERFORMANCE EVALUATION

In this section, we describe the results obtained for the scenarios presented in the previous section. We assume that the total downlink bandwith is 500 MHz and the BSs allocate the power uniformly over this bandwith. The pathloss model is given exploiting the results presented in [8] on the mmWave band. Assuming a system effective noise temperature T equal to 300 K, the one-sided noise power spectral density value results equal to $N_0 = \text{kT} = -143.82$ dBW/MHz, where k is the Boltzmann constant. The detailed system parameters are reported in Table I. All the evaluations have been performed using a customized MATLAB simulator.

A. Single omnidirectional BS

In Fig. 4, we evaluate the region around the FSS where a single omnidirectional BS can be placed without causing I/N to go above the recommended threshold. In particular, the graph shows the contour of the "-10 dB region" that represents the area where a single omnidirectional BS generates an amount of interference at the FSS higher than the regulatory requirements. We evaluate the regions obtained with a pico BS, $P_{BS} = 30$ dBm and with a macro BS, $P_{BS} = 43$ dBm, considering the

Parameter	Value
Carrier frequency	18 GHz
Total downlink bandwidth	500 MHz
BS transmit power	30, 43 dBm
BS antenna height	20 m
BS omnidirectional antenna gain	6, 12 dBi
BSs intersite distance	500 m
BS inter-antenna distance	$\lambda/2$
BS beam codebook cardinality	16
FSS antenna main lobe gain	42.1 dBi
FSS antenna diameter	2.4 m
FSS antenna height	2 m
Elevation angle	$10°, 30°$
Pathloss model	$61.39 + 10 \times 2.47 \log(d)$ [8]
Number of scatterers	3
Noise temperature	300 K
Number of users per BS	10
Recommended I/N level	-10 dB
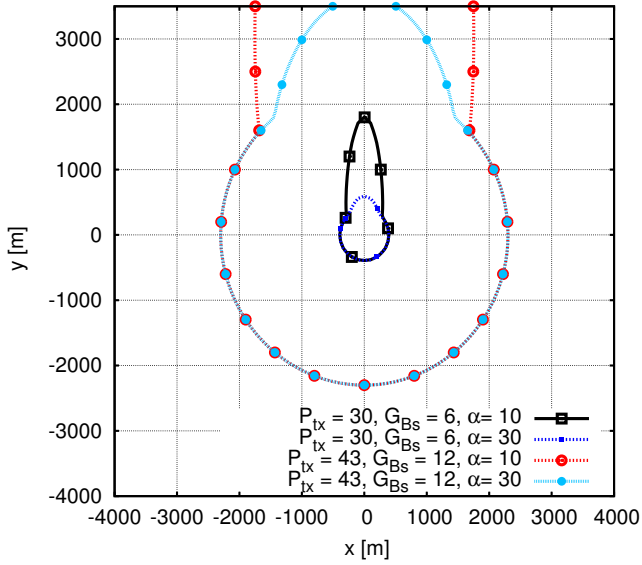
Fig. 4. -10 dB region with a single interferer

FSS elevation angle α equal to $10°$ and $30°$. As expected, the -10 dB area extension is proportional to the BS power. Moreover, the interference depends on the FSS elevation angle, in particular the higher the α the lower the interference at the FSS.

B. Multiple omnidirectional BSs

In the next simulations, we evaluate the interference at the FSS when more omnidirectional pico BSs are deployed around the FSS. In the first simulation, we consider the worst case scenario when one BS within every tier of BSs is placed in the direction of the maximum FSS antenna gain, *i.e.*, $\vartheta = 0°$, and the others are placed accordingly with a fixed intersite distance d_i. Considering the expected cell coverage in next generation cellular networks [5] we assume $d_i = 500$ m. Fig.
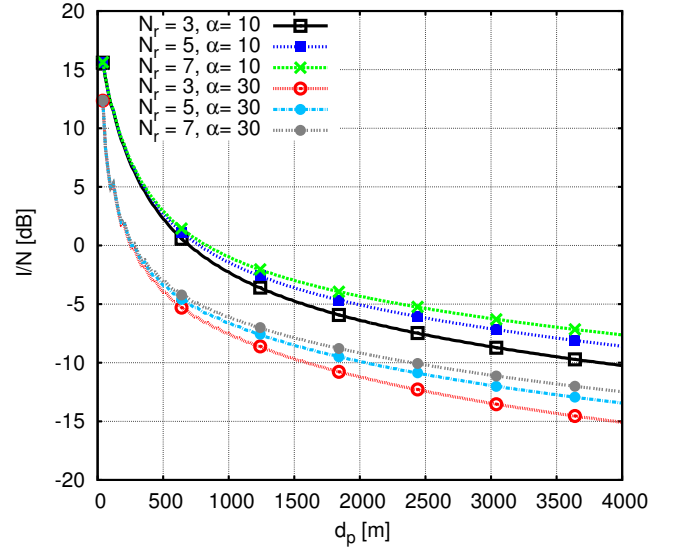

Fig. 5. Aggregate interference in the omnidirectional worst-case scenario

5 shows the I/N obtained varying the protection distance and adopting three different values for the number of BS tiers, N_r, and two different elevation angles. We observe that, for $\alpha = 10°$, the interference at the FSS is very high and the I/N level recommended by the standard is never achieved even for high d_p values. Increasing the elevation angle to $30°$ the recommended value is reached for $d_p = 2000$ m. As expected, considering more BSs circles the interference at the FSS increases but the effects of the more distant BSs circles become negligible due to the high pathloss. Then, in the next evaluations, we restrict the value of N_r to 3 or 5.

Fig. 6 shows the cumulative distribution function (CDF) of I/N when the BSs are deployed randomly over the circles around the FSS. We consider five tiers of BSs and two fixed protection distances for each value of the elevation angle. The intersite distance between the BSs is fixed as in the previous simulation. The results are obtained via Monte Carlo simulation with several runs per configuration where in each run the BS positions are changed. Firstly, we note that since the radiation pattern shape depends on α, the higher the FSS elevation angle the lower the interference generated to the FSS and so the I/N level. In general, for the d_p values considered the interference requirement is never met.

C. Multiple directional BSs

In Figs. 7, 8, and 9 we evaluate the interference at the FSS exploiting an analog beamforming scheme at the BSs that maximizes the user capacity. We consider a random scheduling pattern of the users. Fig. 7 shows the I/N obtained in the worst-case scenario by varying the protection distance and considering different numbers of antennas at the transmitter N_a, and different values of α. The number N_r of tiers of BSs around the FSS is fixed to three and the results have been obtained, as in the previous case, by Monte Carlo evaluations over different channel realizations and user selections. When
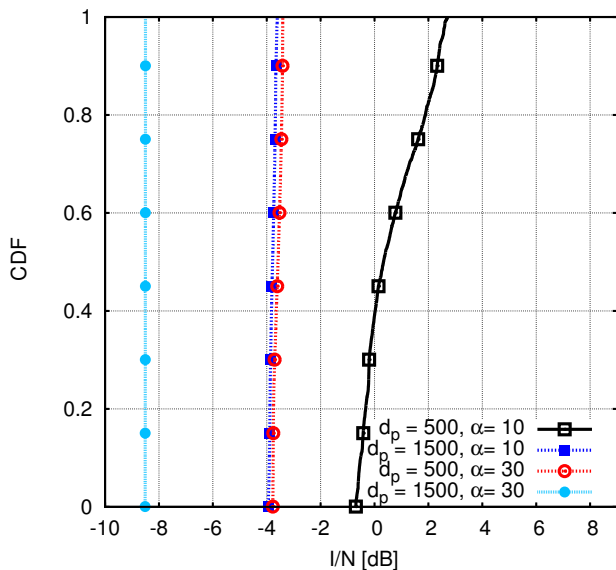
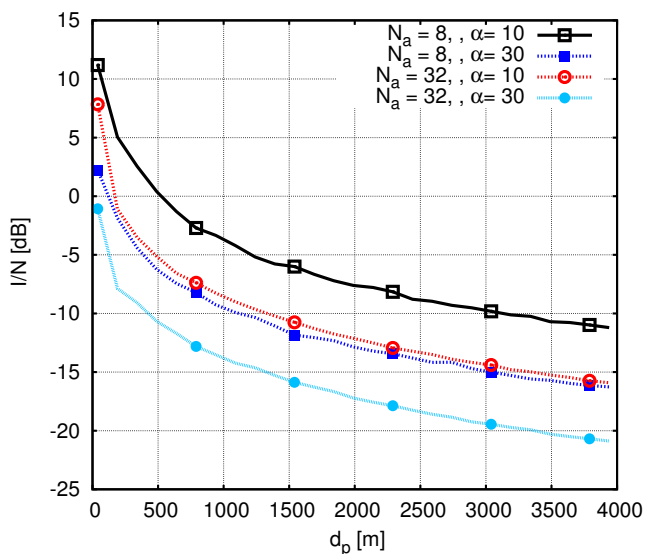Fig. 6. Aggregate interference CDF with omnidirectional BSs

Fig. 8. Aggregate interference CDF considering BSs with $N_a = 16$

Fig. 7. Aggregate interference in the beamforming worst-case scenario
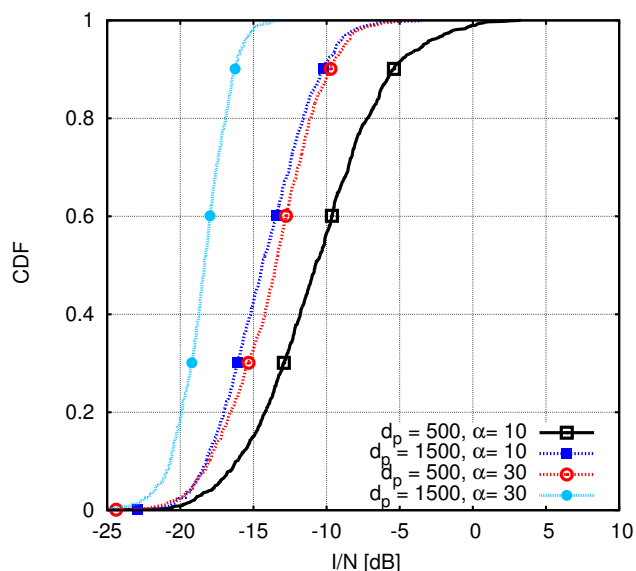
Fig. 9. Aggregate interference CDF considering BSs with $N_a = 64$

the number of antennas is increased, the directional beams become narrower and the interference due to the side lobes decreases. Also, the interference towards the FSS decreases with the number of antennas at the BSs. Besides, we note that the interference due to a small elevation angle can be compensated by using a larger antenna array. In general, beamforming schemes can reach a considerable improvement in comparison with the omnidirectional BSs case.

Fig. 8 shows the CDF of I/N when the number of antennas is set to 16 and the BSs are randomly placed around the FSS over three tiers. Using this configuration, we notice that it is possible to satisfy the standard recommendation constraints adopting a protection distance of 1500 m for an elevation angle equal to
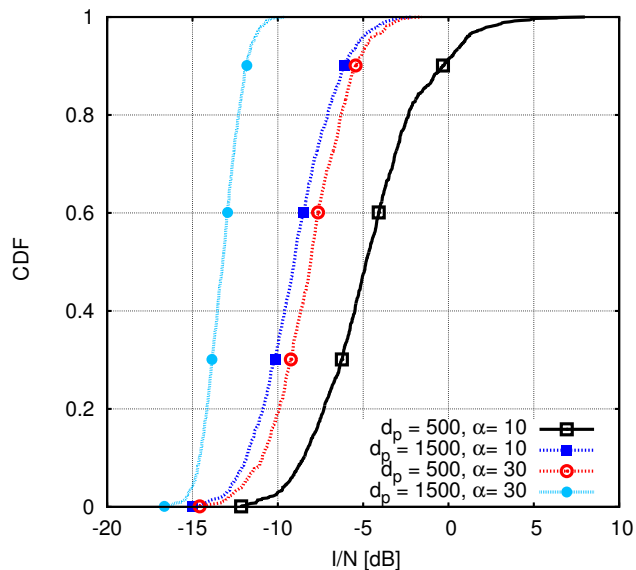
$30°$. We emphasize that user scheduling and beam selection are completely unaware of the interference at the FSS since no communication is assumed between the devices. The results of a similar evaluation are reported in Fig. 9 increasing the number of antennas at the BSs to 64. We note that the required protection distance with $\alpha = 30°$ is reduced to 500 m and the regulatory requirement can be satisfied also for $\alpha = 10°$ with $d_p = 1500$ m.

Fig. 10 shows the impact of the BSs intersite distance on the interference at the FSS. In this evaluation we set $N_a = 16$, $d_p = 1500$, $N_r = 3$ and $\alpha = 30$. As expected, decreasing the intersite distance, the BS density around the FSS increases, thus generating higher interference at the FSS. The BSs density
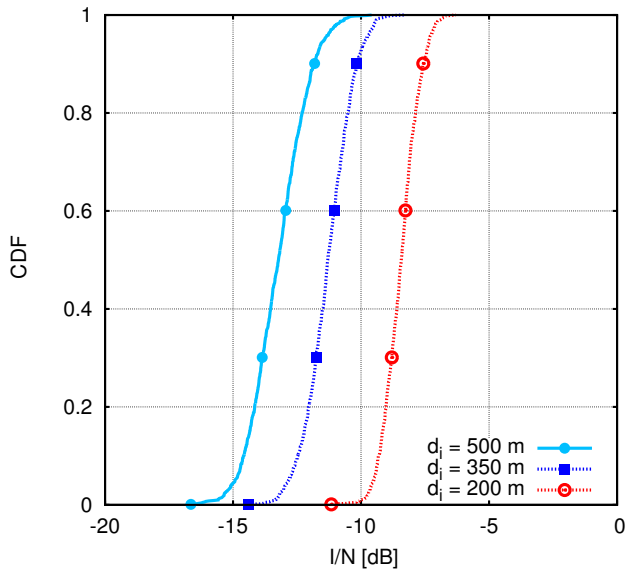
Fig. 10. Aggregate interference CDF considering different BSs intersite distances

is then another key parameter to design the network in order to preserve the FSS functionalities.

IV. CONCLUSIONS AND FUTURE WORK

In this paper, we investigated the coexistence feasibility of FSSs and cellular BSs in a mmWave scenario. We evaluated the I/N at the FSS considering standard parameters and different BS deployments and configurations. In particular, we studied single and aggregate interference scenarios with a random multi-tier distribution of the BSs. Moreover, we analyzed the impact of the introduction of an RF beamforming scheme at the transmitters with the assumption of no interaction among FSS and BSs. From the results obtained, it appears that exploiting the characteristics of the mmWave scenario, such as high pathloss and large antenna arrays, the coexistence of FSSs and BSs in the same area is possible. Moreover, parameters such as the BS density, the protection distance and the FSS elevation angle became crucial in the network deployment to guarantee the FSS functionalities.

As future work, we intend to develop possible distributed cooperative algorithms of beamforming and scheduling among the BSs to mitigate the interference at the FSS. Finally, more complex scenarios such as heterogeneous networks and more realistic BSs deployments could be considered.

ACKNOWLEDGMENT

REFERENCES

[1] Cisco, Cisco Visual Networking Index: Global Mobile Data Traffic Forecast Update, 2013–2018, Feb. 2014, White Paper, pp. 1-40.

[2] T. S. Rappaport, S. Sun, R. Mayzus, H. Zhao, Y. Azar, K. Wang, G. N. Wong, J. K. Schulz, M. Samimi, F. Gutierrez, "Millimeter wave mobile communications for 5G cellular: it will work!," *IEEE Access,* vol. 1, pp. 335–349, 2013.

[3] W. Roh, J. Y. Seol, J. Park, B. Lee, J. Lee, Y. Kim, J. Cho, K. Cheun, F. Aryanfar, "Millimeter-wave beamforming as an enabling technology for 5G cellular communications: theoretical feasibility and prototype results," *IEEE Comm. Mag.,* pp. 106–113, Feb. 2014.

[4] T. Kim, J. Park, J. Seol, S. Jeong, J. Cho, W. Roh, "Tens of Gbps support with mmWave beamforming systems for next generation communications," *IEEE GLOBECOM,* pp. 3685–3690, 9–13 Dec. 2013.

[5] S. Rangan, T. S. Rappaport, E. Erkip, "Millimeter wave cellular wireless networks: potentials and challenges," *Proc. of the IEEE,* vol. 102, no. 3, pp. 366–385, March 2014.

[6] M. R. Akdeniz, Y. Liu, M. K. Samimi, S. Sun, S. Rangan, T. S. Rappaport, E. Erkip, "Millimeter wave channel modeling and cellular capacity evaluation," arXiv preprint arXiv: 1312.4921, 2013.

[7] T. Bai, V. Desai, R. W. Heath, "Millimeter wave cellular channel models for system evaluation," *IEEE ICNC 2014,* pp. 178–182, 3–6 Feb. 2014.

[8] S. Hur, Y. J. Cho, T. Kim, J. Park, A. Molisch, K. Haneda and M. Peter "Wideband Spatial Channel Model in an Urban Cellular Environments At 28 GHz," *Proc. EuCAP 2015,* April 2015.

[9] Metis project, "Intermediate description of the spectrum needs and usage principles," D5.1 Deliverable, Aug. 2013.

[10] CoRaSat project, "Service and market requirememts," D.2.1 Deliverable, Oct. 2013.

[11] ITU-R M.2109, "Sharing studies between IMT advanced systems and geostationary satellite networks in the fixed-satellite service in the 3400-4200 and 4500-4800 MHz frequency bands," 2007.

[12] ITU-R 4-5-6-7/TEMP/139-E, "Sharing and compatibility between IMT system and fixed-satellite service network in 5850-6425 MHz frequency range," Feb. 2007.

[13] S. K. Sharma, S. Chatzinotas, B. Ottersten, "Satellite cognitive communications: Interference modeling and techniques selection," *Proc. SPSC,* pp. 111–118, 5–7 Sept. 2012.

[14] J. Lim, H. Jo, H. Yoon, J. Yook,"Interference mitigation technique for the sharing between IMT-advanced and fixed satellite service," *Journ. of Comm. and Net.,* vol. 9, no. 2, pp. 159–166, June 2007.

[15] D. Oh, S. Lee, D. Ahn, S. Kim, "A Study on the Separation Distance for Frequency Sharing between GSO Network and Terrestrial Network in Ka Band," *Proc. IEEE VTC Spring,* pp. 2967–2971, 11–14 May 2008.

[16] S. K. Sharma, S. Chatzinotas, B. Ottersten, "Transmit beamforming for spectral coexistence of satellite and terrestrial networks," *Proc. IEEE CROWNCOM,* pp. 275–281, 8–10 July 2013.

[17] F. Guidolin, M. Nekovee, L. Badia, M. Zorzi, "A Cooperative Scheduling Algorithm for the Coexistence of Fixed Satellite Services and 5G Cellular Network," *Proc. IEEE ICC 2015.*

[18] ITU-R P.452-15, "Prediction procedure for the evaluation of interference between stations on the surface of the Earth at frequencies above about 0.1 GHz," Sept. 2013.

[19] ITU-R S.465, "Reference radiation pattern for earth station antennas in the fixed-satellite service for use in coordination and interference assessment in the frequency range from 2 to 31 GHz," Jan. 2010.

[20] A. Alkhateeb, O. El Ayach, G. Leus, R. W. Heath, "Hybrid precoding for millimeter wave cellular systems with partial channel knowledge," *Proc. ITA Workshop,* pp. 1–5, 10–15 Feb. 2013.

[21] ITU-R SF.558-2, "Maximum allowable values of interference from terrestrial radio links to systems in the fixed-satellite service employing 8-bit PCM encoded telephony and sharing the same frequency bands," July 1986.

[22] ITU-R Rec. S.1432, "Apportionment of the allowable error performance degradation to Fixed-Satellite Service (FSS) hypothetical reference digital paths arising from time invariant interference for system operating below 30 GHz," Jan. 2000.